

An Experimental Model-Based Exploration of Cytokines in Ablative Radiation-Induced Lung Injury In Vivo and In Vitro

Zhen-Yu Hong · Kwang Hyun Song ·
Joo-Heon Yoon · Jaeho Cho · Michael D. Story

Received: 23 October 2014 / Accepted: 26 February 2015 / Published online: 7 March 2015
© Springer Science+Business Media New York 2015

Abstract

Introduction Stereotactic ablative radiotherapy is a newly emerging radiotherapy treatment method that, compared with conventionally fractionated radiation therapy (CFRT), allows an ablative dose of radiation to be delivered to a confined area around a tumor. The aim of the present study was to investigate the changes of various cytokines that may be involved in ablative radiation-induced lung injury in vitro and in vivo.

Methods In the in vivo study, ablative-dose radiation was delivered to a small volume of the left lung of C3H/HeJCr mice using a small-animal irradiator. The levels of 24

cytokines in the peripheral blood were tested at several time points after irradiation. For the in vitro study, three mouse cell types (type II pneumocytes, alveolar macrophages, and fibroblasts) known to play important roles in radiation-induced pneumonitis and lung fibrosis were analyzed using a co-culture system.

Results In the in vivo study, we found obvious patterns of serum cytokine changes depending on the volume of tissue irradiated (2-mm vs. 3.5-mm collimator). Only the levels of 3 cytokines increased with the 2-mm collimator at the acute phase (1–2 weeks after irradiation), while the majority of cytokines were elevated with the 3.5-mm collimator. In the in vitro co-culture system, after the cells were given an ablative dose of irradiation, the levels of five cytokines (GM-CSF, G-CSF, IL-6, MCP-1, and KC) increased significantly in a dose-dependent manner.

Conclusions The cytokine levels in our radiation-induced lung injury model showed specific changes, both in vivo and in vitro. These results imply that biological studies related to ablative-dose small-volume irradiation should be investigated using the corresponding experimental models rather than on those simulating large-volume CFRT.

The authors dedicate this article to the late Dr. Reinhard Kodym.

Electronic supplementary material The online version of this article (doi:10.1007/s00408-015-9705-y) contains supplementary material, which is available to authorized users.

Z.-Y. Hong · J. Cho (✉)

Department of Radiation Oncology, Yonsei University College of Medicine, 50 Yonsei-ro, Seodaemun-gu, Seoul 120-752, South Korea
e-mail: jjhmd@yuhs.ac

Z.-Y. Hong

Department of Medical Oncology, The First Affiliated Hospital of Xinxiang Medical University, Weihui, Henan Province, China

K. H. Song · M. D. Story (✉)

Division of Molecular Radiation Biology, Department of Radiation Oncology, University of Texas Southwestern Medical Center, 2201 Inwood Rd, Dallas, TX 75093, USA
e-mail: michael.story@utsouthwestern.edu

J.-H. Yoon

Department of Otorhinolaryngology, BK 21 Project for Medical Sciences, Yonsei University College of Medicine, Seoul, South Korea

Keywords Stereotactic ablative radiotherapy · Cytokine · Radiation pneumonitis · Radiation fibrosis · Small-animal model

Introduction

Stereotactic ablative radiotherapy (SABR) is a newly emerging radiotherapy treatment method that, compared with conventionally fractionated radiation therapy (CFRT), allows an ablative dose of radiation to be delivered to a confined area around a tumor. SABR has been applied to

the treatment of early-stage lung cancers in inoperable patients with excellent clinical results [1], and this approach to radiotherapy is being widely adopted and has the potential to represent a feasible alternative to surgery for early-stage operable populations.

Considering the tremendous potential of SABR, investigations of the underlying radiobiology pertaining to ablative dose-per-fraction therapy is of paramount importance, owing to the risks of severe adverse effects in normal tissue, particularly when insufficient consideration is given to the normal tissue dose and the type of normal tissue present in the radiation field. The response of tissues to such regimens is likely to be very different from the response to CFRT [2–6], and it is important to understand the underlying radiobiology in order to provide a rationale for the use of ablative dose-per-fraction therapeutic regimens [7]. Toward this goal, small animal platforms have been developed to simulate SABR delivery [8–10]. Moreover, in addition to animal models, an *in vitro* model of ablative-dose radiation-induced lung inflammation would be useful.

The response to ionizing radiation involves a number of mediators, including inflammatory cytokines produced by macrophages, epithelial cells, and fibroblasts [11]. Since the inflammatory and fibrogenic processes associated with radiation-induced lung injury are initiated and sustained by a complex cytokine network [12], the ability to simultaneously quantify multiple cytokines is critical for deciphering how they affect radiation-induced lung toxicity. A cytokine that displays differences after the completion of SABR but before the clinical onset of radiation-induced lung injury would be useful for the early diagnosis of radiation pneumonitis. In addition, such a cytokine might serve as a diagnostic tool to distinguish radiation pneumonitis from other possible diagnoses (infectious pneumonia, tumor progress, lymphangitic spread, and deteriorated chronic obstructive pulmonary disease). Further, this cytokine marker would allow for timely initiation of the appropriate treatment, as delayed administration of steroid hormones often worsens the prognosis for patients with radiation-induced pneumonitis [13].

In our previous studies [8], we established an experimental model and image-guided animal irradiation system for the study of ablative dose-per-fraction irradiations. It was designed to provide the mouse lung a small volume, analogous to that used in SABR for human beings. In the present report, we investigated the cytokine changes in the blood of mice after delivering ablative-dose small-volume irradiation (ADSVI) to the lung using the same irradiation system. Moreover, we attempted to establish an *in vitro* model in which three cell types (type II pneumocytes, alveolar macrophages, and fibroblasts) were co-cultured, and investigated the cytokine changes after

delivering ablative radiation to these cells. Our ultimate goal is to understand the pattern of cytokine changes upon SABR so that this therapy can be optimized to limit the adverse effects in normal tissues.

Materials and Methods

A complete description of the materials and methods is available in this article's online supplement.

Mouse Irradiation

High-dose radiation was delivered to a small volume of the left lung of C3H/HeJCr mice using a small-animal stereotactic irradiator. The detailed description of high dose-per-fraction irradiation of limited lung volumes simulating SABR regimens in a small-animal model can be found in Ref. [8]. To mimic SABR conditions by irradiating only a small volume, 2 and 3.5-mm collimators were used, with a dose of 90 Gy administered to the left lungs of the mice.

Histopathologic Examination and Fibrosis Quantification

The mouse lung tissues were prepared in paraffin blocks, and the slides were stained with Masson's Trichrome to evaluate the extent of radiation-induced fibrosis.

Cytokine Measurement

The cytokine concentrations in the serum were assayed using a Bio-Plex ProTM Mouse Cytokine 23-plex Assay Kit (Bio-Rad, Hercules, CA). Because TGF- β 1 was not included in this kit, a separate TGF- β 1 assay kit was purchased from Assay Design[®] (Farmingdale, NY, USA).

Cell Lines and Reagents

Mouse embryonic fibroblast (NIH/3T3), alveolar macrophage (MHS), and type II alveolar epithelial cell lines (MLE-12) were purchased from ATCC (Manassas, VA, USA). MLE-12, NIH/3T3, and MHS cells were stained with red, green, and blue cell trackers, respectively, which are fluorescent probes retained in living cells through several generations. After staining with the relevant cell tracker, the cells were mixed in a 1:1:1 proportion. Subsequently, the mixed cells were co-cultured for 12 h. Next, the cells were subjected to 20-Gy irradiation. 24 h later, the cells were separated using fluorescence-activated cell sorting (FACS) according to the different emitted wavelengths.

FACS

The MLE-12, NIH/3T3, and MHS cells absorbed 355, 488, and 561 nm light, and were separated by the emitting wavelengths, which were 450 ± 25 , 525 ± 25 , and 610 ± 10 nm, respectively.

Polymerase Chain Reaction (PCR)

Information about mRNA extraction, cDNA synthesis, primer sequences, electrophoresis, cycling conditions, and other processes is available in this article's online supplement.

Statistics

Data were statistically analyzed using the Student's *t* test, and differences with a *P* value of <0.05 were considered significant.

Results

Comparison of Radiation-Induced Fibrosis with Different Irradiation Volumes

After applying ADSVI to the peripheral lung, the mice were sacrificed in order to detect collagen depositions. A focal injury area was observed in the left lung of the mice (Fig. 1b). A slight collagen deposition was noted from week 2 after irradiation, and overt collagen depositions were observed at weeks 6 and 12 after irradiation. In order to investigate whether the irradiation volume had any effect on the progression of fibrosis, the fibrosis scores were analyzed upon irradiation with 2 and 3.5-mm collimators. As shown in Fig. 1c, there were no significant differences between the two volumes in terms of fibrosis, at any time point.

Cytokine Levels in the Serum from Irradiated Mice

The cytokine levels in the blood of mice irradiated with 2 and 3.5-mm collimators exhibited large individual differences that resulted in significant variance for the entire group. However, obvious patterns of cytokine change were observed. In the serum extracted from animals irradiated with the 2-mm collimator, three cytokines were increased at week 1 and/or 2 compared to the control ($p < 0.05$, Fig. 2a), and two cytokines were increased at 6 weeks compared to at 2 weeks ($p < 0.05$, Fig. 2b). The other cytokines did not show significant changes (Fig. 2c). However, in the animals irradiated with the 3.5-mm

collimator, most cytokines showed significant increases at 1 or 2 weeks compared to the controls ($p < 0.05$, Fig. 3a). Furthermore, IL-3 was elevated at 6 and 12 weeks when compared to its level at 2 weeks ($p < 0.05$, Fig. 3b). IL-1 α and IL-9 were decreased at 12 weeks ($p < 0.05$, Fig. 3c), and three cytokines showed no significant changes over the entire period ($p > 0.05$, Fig. 3d).

Cytokine Levels in Irradiated Mouse Cell Lines

It is well known that macrophages, epithelial cells, and fibroblasts are the most important producers of cytokines that directly or indirectly induce inflammation and fibrosis in irradiated lungs [11]. To establish an in vitro model reflecting SABR-induced lung injury as much as possible, three cell lines, namely NIH/3T3, MHS, and MLE-12, were selected. The cytokine secretion levels in the supernatant of the co-cultures of these cell lines or from each cell line individually, with or without irradiation, were evaluated. The results are shown in Table 1. The data showed some interesting trends: (1) most cytokines could not be detected in MLE-12 and NIH/3T3 cells cultured alone; (2) all cytokines could be detected in the co-cultures of the three cell lines, and these levels were much higher than those in the MHS cells alone; (3) nearly half of the cytokines could be detected at intermediate or high levels in the co-cultured cells (≥ 100 pg/ml), with many of these cytokines known to attract macrophages, neutrophils, and eosinophils [14]; and (4) the secretion levels of most cytokines in the MHS cells post-irradiation could be detected to variable degrees, suggesting a typical immune cell character of these cells. It is well known that macrophages, epithelial cells, and fibroblasts are the most important producers of cytokines that directly or indirectly induce inflammation and fibrosis in irradiated lungs [11]. To establish an in vitro model reflecting SABR-induced lung injury as much as possible, three cell lines, namely NIH/3T3, MHS, and MLE-12, were selected. The cytokine secretion levels in the supernatant of the co-cultures of these cell lines or from each cell line individually, with or without irradiation, were evaluated. The results are shown in Table 1. The data showed some interesting trends: (1) most cytokines could not be detected in MLE-12 and NIH/3T3 cells cultured alone; (2) all cytokines could be detected in the co-cultures of the three cell lines, and these levels were much higher than those in the MHS cells alone; (3) nearly half of the cytokines could be detected at intermediate or high levels in the co-cultured cells (≥ 100 pg/ml), with many of these cytokines known to attract macrophages, neutrophils, and eosinophils [14]; and (4) the secretion levels of most cytokines in the MHS cells post-irradiation could be detected to variable degrees, suggesting a typical immune cell character of these cells.

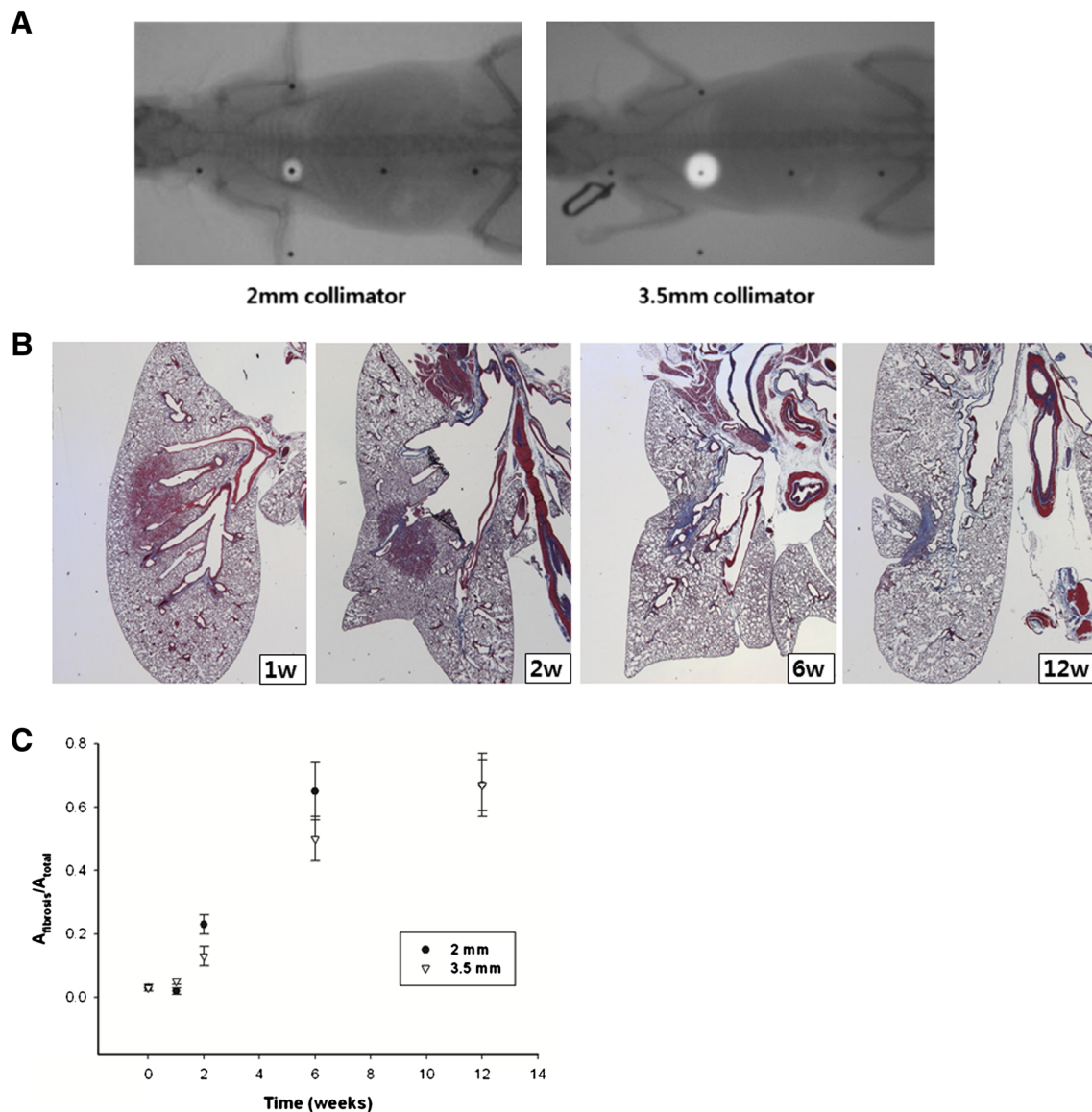


Fig. 1 Comparison of radiation-induced fibrosis with different irradiation volumes. **a** Image-guided localization of the radiation area. **b** The lung sections were stained with Masson's trichrome to visualize collagen depositions. Representative micrographs ($\times 12.5$

magnification) of the irradiated area are shown at each time point. **c** Comparison of fibrosis intensity in areas of the mouse lungs irradiated with 2 and 3.5-mm collimators

Among the 24 cytokines assessed, five cytokines, namely IL-6, G-CSF, GM-CSF, KC, and MCP-1, showed significant increases in a dose-dependent manner ($p < 0.05$; Table 2). The changes in these five cytokine levels in the single- and co-cultured media are shown in detail in Fig. 4. In the co-cultured system, after the cells were irradiated with the indicated doses, the levels of these five cytokines increased in a dose-dependent manner to 40 Gy; however, there was a diminished rate of response at 100 Gy, suggesting that the culture's ability to express cytokines was near saturation.

Gene Regulation of Cytokines in Each Irradiated Mouse Cell Line in Co-culture Conditions

In order to investigate which cell line was more responsible for secreting specific cytokines in the co-culture system, we used FACS to separate the cell lines before and after radiation. In a previous experiment investigating the dose-effect relationship in the co-culture system (Fig. 4), we found that the ED50 (50 % effective dose) was approximately 20 Gy (data not shown). Therefore, in this experiment, we selected 20 Gy for further investigating the

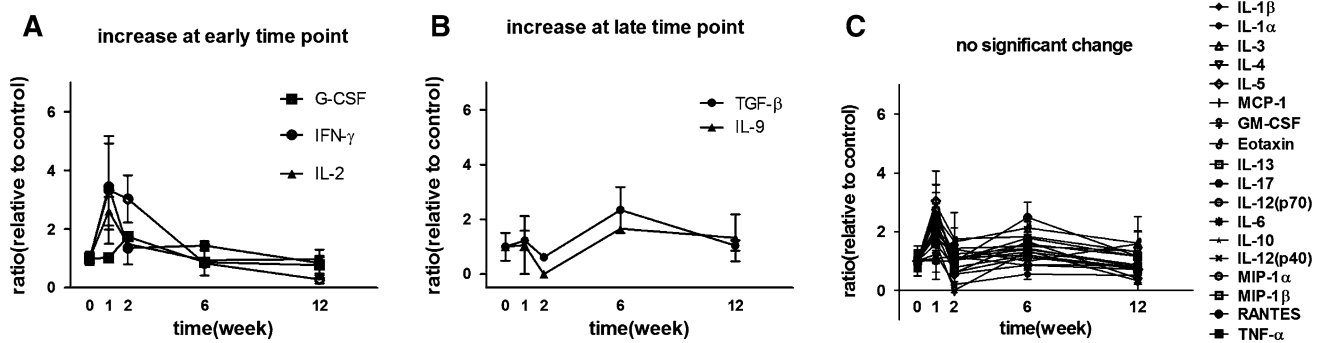
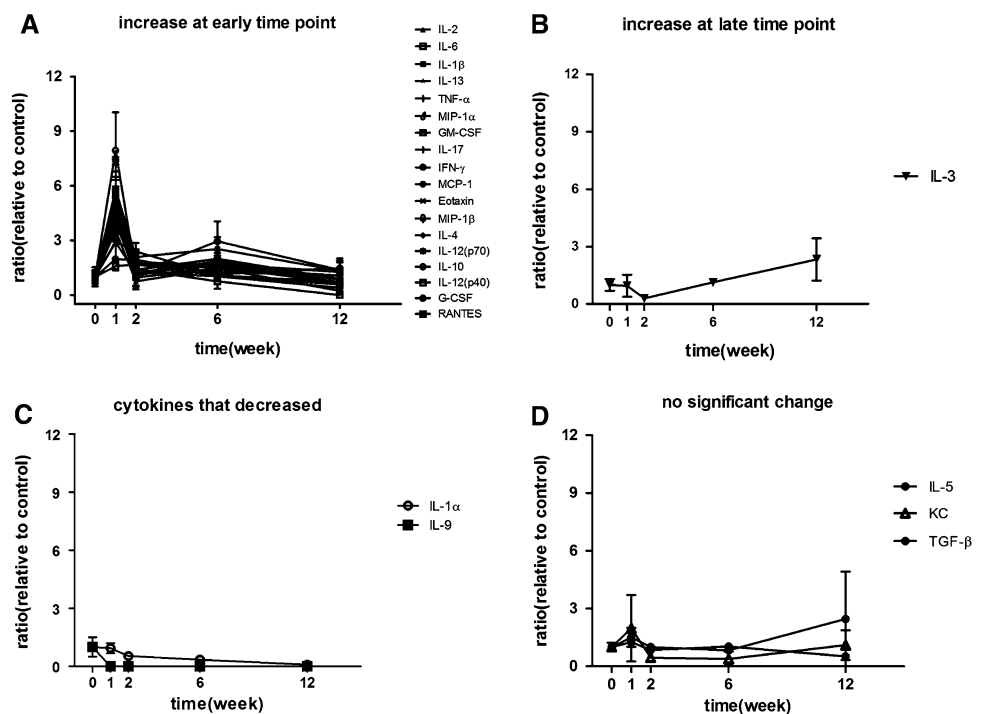


Fig. 2 Cytokine levels in the mouse serum after irradiation using a 2-mm collimator. A dose of 90 Gy was administered to the left mouse lung in one fraction. A 2-mm collimator was applied to produce focal irradiation beams. The levels of 24 cytokines in the peripheral blood were evaluated at the indicated time points after irradiation. **a** G-CSF

was increased at 2 weeks compared to the control ($p < 0.05$), while the IFN- γ and IL-2 levels were increased at 1 week compared to the control ($p < 0.05$). **b** Cytokines increased at 6 weeks compared to 2 weeks ($p < 0.05$). **c** Cytokines that did not show significant changes between any time points

Fig. 3 Cytokine levels in the mouse serum after irradiation using a 3.5-mm collimator. A dose of 90 Gy was administered to the left mouse lung in one fraction. A 3.5-mm collimator was applied to produce focal irradiation beams. The levels of 24 cytokines in the peripheral blood were evaluated at the indicated time points after irradiation. **a** IL-12 (p40) and G-CSF were increased at 2 weeks compared to the control ($p < 0.05$), while all other cytokine levels were increased at 1 week compared to the control ($p < 0.05$). **b** IL-3 was increased at the late time point compared to week 2 ($p < 0.05$). **c** Cytokines that were decreased at week 12 compared to the control ($p < 0.05$). **d** Cytokines that did not show significant changes



gene regulation of cytokines in each irradiated cell line. The mRNA expression levels for specific cytokines were determined by reverse transcriptase-PCR (Fig. 5). We found that the mRNA levels of IL-6, GM-CSF, and G-CSF were up-regulated in MLE-12 and MHS cells, whereas, in contrast, KC mRNA was up-regulated in the NIH/3T3 and MLE-12 cells. Moreover, all cell types in the co-culture system expressed MCP-1 mRNA, but only showed minor differences in the expression levels before and after irradiation. Interestingly, amongst the three cell lines, GM-CSF mRNA was expressed at the highest levels in MHS cells before irradiation, whereas after irradiation, MLE-12 cells showed the highest levels of GM-CSF mRNA.

Discussion

To date, many studies have evaluated the changes in cytokine levels after delivering low-dose large-volume irradiation to the whole mouse lung, simulating clinical CFRT [15–18]; however, to our knowledge, no study has yet investigated the changes in the serum cytokine levels in response to ADSVI to the mouse lung, which simulates clinical SABR. In this study, the pro-inflammatory cytokines that may potentially be involved in ADSVI-induced lung injury were investigated in vitro and in vivo.

Cytokine changes in the peripheral blood are considered dependent on the radiation dose to the lung [19–21].

Table 1 Cytokine secretion profile of alveolar macrophages, type II pneumocytes, fibroblasts, and their mixture in response to irradiation

	Cell Lines	IL-1 α	IL-1 β	IL-2	IL-3	IL-4	IL-5	IL-6	IL-9	IL-10	IL-12(p40)	IL-12(p70)	IL-13	IL-17	Eotax-in	G-CSF	GM-CSF	IFN- γ	KC	MCP-1	MIP-1 α	MIP-1 β	RANTES	TNF- α	TGF- β
Tiny secretion (< 10 pg/ml)	MH-S	■	■	■	■			■		■	■	■	■					■	■					■	
	MLE-12							■			■	■		■											
	NIH-3T3										■	■												■	
	MIX	■	■	■	■	■	■	■			■	■	■	■					■					■	■
Low secretion (≥ 10 & < 100 pg/ml)	MH-S		■						■																
	MLE-12																							■	
	NIH-3T3										■	■							■						
	MIX							■	■	■	■	■													
Intermediate secretion (≥ 100 & < 1000 pg/ml)	MH-S										■	■			■								■		■
	MLE-12																			■	■				
	NIH-3T3										■	■													■
	MIX										■	■	■	■	■	■									■
High secretion (≥ 1000 pg)	MH-S																			■	■	■	■		
	MLE-12																				■	■			
	NIH-3T3																				■	■	■	■	
	MIX																			■	■	■	■	■	
Undetectable (Out of Range, low)	MH-S					■																			
	MLE-12	■	■	■	■	■	■	■	■	■	■	■	■	■	■	■	■	■	■	■	■	■	■	■	■
	NIH-3T3	■	■	■	■	■	■	■	■	■	■	■	■	■	■	■	■	■	■	■	■	■	■	■	■
	MIX	■	■	■	■	■	■	■	■	■	■	■	■	■	■	■	■	■	■	■	■	■	■	■	■

NIH/3T3, MHS, and MLE-12 cells were either cultured alone (15 × 10⁴ cells of each cell line in each well) or mixed together (5 × 10⁴ cells of each cell line in one well) in 6-well dishes. An irradiation dose of 100 Gy was administered to these cells. The cytokine secretion levels in the supernatant of the co-cultures and from each individual cell line were evaluated. The values were divided into 5 groups according to the range of concentration in order to assess the trend of distribution. ■ Tiny secretion (< 10 pg/ml), ■ Low secretion (≥ 10 < 100 pg/ml), ■ Intermediate secretion (≥ 100 < 1000 pg/ml), ■ High secretion (≥ 1000 pg), ■ Undetectable (out of range, low)

Greater the irradiation delivered to the lung, the more pronounced are the cytokine changes observed. However, since, in most cases, radiotherapy is performed on the whole lung, little is currently known regarding the effects of volume on the cytokine levels. In this study, we determined the blood levels of 24 cytokines after 90 Gy of radiation delivered with different small volumes to the left lung of C3H/HeJCr mice. In our previous study [8], we found that 100 Gy irradiation resulted in the experimental mice dying as a result of whole left lung consolidation and pleurisy (autopsy finding), while 40 Gy was not high enough to induce fibrosis in the early phase. Furthermore, in other previous studies by our group [22, 23], we found that a dose of 90 Gy was well tolerated in the mice, and typical histopathological events of lung injury were exhibited in our mouse model within 12 weeks after delivering the irradiation. Therefore, in the present study, we selected 90 Gy as the highest dose for investigating fibrosis. Furthermore, because the cytokine levels exhibited large individual differences that resulted in significant

variance for the entire group, we tried to emphasize the trend of cytokine changes in this study. Interestingly, using a 3.5-mm collimator, most cytokines were dramatically increased at 1 week after irradiation. Although there was no significant difference for most cytokine levels when using a 2-mm collimator, their mean value also increased at 1 week. These findings suggest that ADSVI-induced cytokine elevation occurs early, and that pro-inflammatory cytokines are sensitive to the radiation volume used.

In addition to the unique trend observed in the cytokine level changes, the individual cytokine levels in our small-volume ablative-dose system also differed from that observed using CFRT-simulating models. In a previous study, the cytokine levels in the blood were compared between C57BL/6 and C3H mice at several time points within 1 week of receiving low-dose whole-lung irradiation [14]. In that study, although some cytokines, including G-CSF, IL-6, KC, and MCP-1, showed transient elevation, they all recovered to normal levels after 1 week. On the other hand, in our ADSVI system, these

Table 2 Radiation dose-responses on cytokine secretions after irradiation in the co-culture

Mixed	0 Gy Mean ± Std	10 Gy Mean ± Std	20 Gy Mean ± Std	40 Gy Mean ± Std	100 Gy Mean ± Std	<i>p value</i> [†]
IL-1a	4.61 ± 0.99	4.54 ± 0.59	5.44 ± 0.91	6.67 ± 0.91	4.65 ± 0.74	0.0833
IL-1b	4.36 ± 4.86	4.31 ± 4.78	6.50 ± 7.23	3.79 ± 4.19	4.04 ± 4.48	0.3500
IL-2	*1.63 ± 1.02	*0.82 ± 0.70	*0.82 ± 0.70	*1.43 ± 0.59	*1.43 ± 0.59	0.9500
IL-3	3.13 ± 0.38	2.74 ± 0.48	3.44 ± 0.13	3.30 ± 0.08	3.74 ± 0.82	0.1333
IL-4	OOB < ±	*0.05 ±	OOB < ±	*1.03 ± 0.46	*1.84 ± 0.97	0.3333
IL-5	4.57 ± 1.03	4.57 ± 1.51	4.18 ± 0.51	*2.82 ± 1.44	*2.82 ± 1.44	0.0167
IL-6	53.66 ± 2.97	60.40 ± 2.60	74.15 ± 1.10	84.15 ± 4.64	105.55 ± 1.62	0.0167
IL-9	22.33 ± 15.91	13.13 ± 6.11	16.97 ± 11.49	22.33 ± 5.85	32.10 ± 11.17	0.3500
IL-10	19.71 ± 2.72	20.38 ± 3.38	15.53 ± 0.71	14.28 ± 1.05	13.94 ± 2.59	0.0833
IL-12(p40)	274.88 ± 39.90	265.12 ± 47.95	291.42 ± 18.71	307.68 ± 60.02	307.17 ± 8.89	0.1333
IL-12(p70)	7.96 ± 1.00	7.07 ± 1.63	8.07 ± 0.45	8.18 ± 0.59	7.46 ± 1.09	0.7833
IL-13	106.78 ± 9.75	108.17 ± 7.11	89.46 ± 5.18	89.46 ± 5.18	73.71 ± 15.52	0.0833
IL-17	*1.62 ± 0.81	*1.89 ± 0.38	*2.01 ± 0.87	*2.31 ± 0.38	3.17 ± 0.39	0.0167
Eotaxin	612.22 ± 100.86	443.83 ± 131.10	537.40 ± 109.53	443.83 ± 90.89	570.15 ± 121.79	0.7833
G-CSF	101.37 ± 4.17	121.94 ± 5.73	172.53 ± 9.07	192.56 ± 2.37	228.42 ± 6.55	0.0167
GM-CSF	21.11 ± 3.25	25.21 ± 1.58	26.00 ± 0.34	34.57 ± 2.58	38.82 ± 4.45	0.0167
IFN-γ	*1.80 ± 0.14	*0.94 ± 0.71	*1.22 ± 0.57	*1.22 ± 1.09	*1.63 ± 1.70	0.9500
KC	1276.43 ± 48.79	1363.26 ± 131.46	1675.46 ± 156.80	1960.39 ± 151.14	2310.01 ± 245.46	0.0167
MCP-1	33,296.24 ± 5289.70	33,390.62 ± 5833.95	39,965.47 ± 4295.53	52,808.44 ± 15,000.98	59,894.17 ± 8874.78	0.0167
MIP-1a	5934.13 ± 469.46	5309.65 ± 489.60	5279.94 ± 70.56	6123.30 ± 655.62	5468.52 ± 472.42	0.9500
MIP-1b	5634.33 ± 776.06	4007.77 ± 116.95	3088.55 ± 151.81	2954.03 ± 196.17	2245.02 ± 101.83	0.1170
RANTES	1289.63 ± 38.47	1345.05 ± 168.01	1353.58 ± 44.13	1337.16 ± 94.44	1331.62 ± 83.93	0.9500
TNF-α	OOB < ±	*1.02±	*6.06 ± 2.06	OOB < ±	*6.64 ± 5.76	0.3500
TGF-β	460.04 ± 140.50	364.62 ± 69.93	384.79 ± 77.82	348.59 ± 80.35	398.05 ± 68.72	0.2850

Three cell lines, namely MHS, MLE-12, and NIH-3T3, were cultured together in one cell culture dish. Irradiation doses of 10, 20, 40, and 100 Gy were administered to these cells. The levels of cytokines secreted by these cell lines into the supernatant were evaluated 24 h after irradiation

Bold values are statistically significant ($p < 0.05$)

OOB out of range, OOB> out of range above, OOB< out of range below

* Value extrapolated beyond the standard range

[†] Correlation analysis tested by Spearman's rho

cytokines were dramatically elevated 1 week after irradiation with a 3.5-mm collimator.

It is well known that TGF-β1 plays a central role in fibroblast activation and modulation of the immune response [24, 25]. It has been reported that, after lung irradiation in mice, the TGF-β1 mRNA levels are increased 8 weeks after treatment with 5 and 12.5 Gy, as well as at 26 weeks after treatment with 12.5 Gy [26]. In our study, the protein level of TGF-β1 in the peripheral blood was evaluated after an ablative dose of radiotherapy was administered, and was found to respond much earlier than that reported in the previous study. TGF-β1 increased at 1 week after irradiation with both collimators and again at 6 or 12 weeks (with the 2 and 3.5-mm collimators, respectively). Interestingly, the first increase in the TGF-β1 level was observed 1 week earlier than a slight collagen

deposition was detected (week 3 after irradiation; Fig. 1b). This suggests that there is a lag period between TGF-β1 elevation and TGF-β1-mediated fibrosis formation after irradiating with 90 Gy. Besides TGF-β1, an imbalance in Th1/Th2 cytokine production is also involved in the pathogenesis of pulmonary fibrosis [27]. Recent research has shown that Th1 cytokines such as IL-12 and IFN-γ inhibit fibrocyte differentiation [28, 29] and promote normal tissue repair by limiting fibroblast proliferation, differentiation, and collagen synthesis [30, 31], whereas Th2 cytokines such as IL-4 and IL-10 conversely promote fibrocyte differentiation [32] and regulate fibrotic tissue repair by augmenting fibroblast proliferation and collagen production [33, 34]. In our in vivo study, we found that the volume of SABR was able to influence the Th1/Th2 balance. Small-volume SABR led to the shift in the Th1/Th2

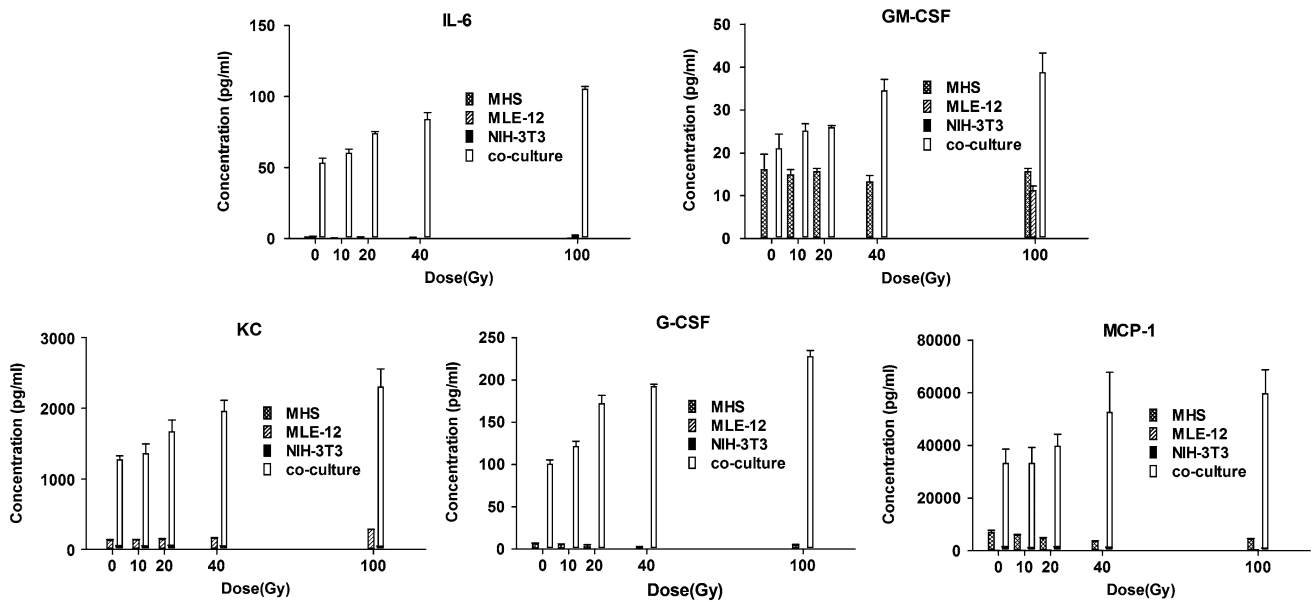


Fig. 4 Cytokine levels that showed a radiation-dose response. Three cell lines, namely MHS, MLE-12, and NIH-3T3, were either cultured alone or together in one cell culture dish. Irradiation doses of 10, 20, 40, and 100 Gy were administered to these cells. The levels of

cytokines secreted by these cell lines into the supernatant were evaluated 24 h after irradiation. Each experiment was performed in triplicate

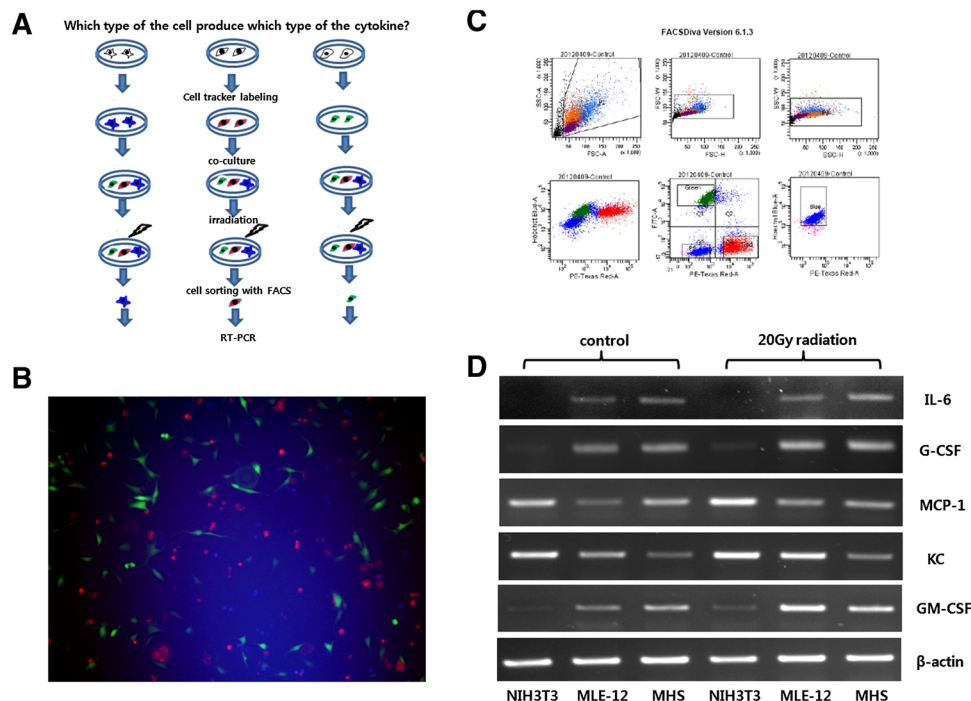


Fig. 5 Gene regulation of cytokines in each irradiated mouse cell line in the co-culture system. **a** Schema of the experimental process. Three cell lines were cultured alone, and each cell line was stained with a different fluorescent cell tracker. These cells were then co-cultured in one cell culture dish. 24 h after 20 Gy of irradiation was administered to these cells, they were separated with fluorescence-activated cell sorting (FACS) according to the emitting wavelengths. mRNA was extracted from the sorted cells, and reverse transcriptase polymerase chain reaction (RT-PCR) was performed. **b** The cell tracker staining

was confirmed by fluorescent microscopy using different wavelength filters before performing FACS. Three images from each wavelength were merged. **c** 24 h after irradiation, the cells stained with cell trackers could still be separated according to the different emitting wavelengths. The cells were gated as indicated and collected in individual tubes. **d** RT-PCR was performed with mRNA extracted from the cells collected from each individual tube after FACS. Each experiment was performed in triplicate

balance toward Th1 dominance at an early time point (IFN- γ in Fig. 2a), and this might explain why a smaller area of fibrosis was induced in these mice. On the other hand, compared to the 2-mm collimator, large-volume irradiation (3.5-mm collimator) induced Th2 cytokine increases at the early time point (IL-4, IL-10 in Fig. 3a), potentially accounting for the large area of fibrosis.

In addition to the *in vivo* model, we also investigated cytokine changes using an *in vitro* model in this study. Interestingly, compared to cytokines from separately cultured cells, most cytokines could be detected at higher levels in the co-cultured cells exposed to irradiation (Table 1). Another interesting finding is that some cytokines (KC, MCP-1, MIP-1 α , MIP-1 β , RANTES) related to macrophage stimulation [14] increased to high levels (≥ 1000 pg/ml; Table 1), which supports the observation that foamy macrophages accumulate in areas of radiation injury in the lungs in humans [35]. Furthermore, among the 24 cytokines assessed, the secretion levels of five cytokines (IL-6, G-CSF, GM-CSF, KC, and MCP-1) increased in a dose-dependent manner. These five cytokines are known to play important roles in inflammation and fibrosis, and it has been reported that MCP-1 and IL-6 contribute to excessive collagen deposition via the recruitment of fibrocytes [13, 36], which are believed to represent a source of fibroblasts and myofibroblasts during the fibro-proliferative response to tissue damage [13, 37]. Moreover, in mice, serum factors such as G-CSF, IL-6, and KC have been explored as potential surrogate markers to predict and detect radiation-induced lung fibrosis, as the serum and tissue levels of these cytokines positively correlate [14]. It is worth noting that increases of these five cytokines were also detected at the early time point in the SABR *in vivo* study (Figs. 2c, 3a), and the significant fibrosis observed histologically (Fig. 1b) is likely related to the increase of these five cytokines.

Insights into the molecular mechanisms of radiation-induced lung injury might provide new strategies for the treatment of radiation pneumonitis. Although we found that the five above-mentioned cytokine levels (IL-6, G-CSF, GM-CSF, KC, MCP-1) increased in the co-culturing system, we were unable to determine which cell lines produced which cytokines. To address this problem, we extracted mRNA after FACS of the three different cell types from the co-cultures and determined which cytokine genes were up-regulated in which cell line before and after irradiation (Fig. 5). Brach et al. [38] previously reported that a temporal increase of IL-6 production by fibroblasts, peaking at 9 h after irradiation, was not irradiation dose-dependent. Conversely, we interestingly found that the cytokine level of IL-6 increased in a dose-dependent manner (Fig. 4) and that this increase was mainly attributed to epithelial cells and macrophages rather than fibroblasts (Fig. 5d). These discrepancies are probably caused by several reasons. First, the potential of cytokine generation in these

three cell lines was amplified by inter-cellular interactions following irradiation in the co-culturing system. Second, IL-6 may be preferentially produced by epithelial cells and macrophages rather than fibroblasts. Third, secretion of IL-6 responds more sensitively to an ablative dose than low doses of irradiation. On the other hand, unlike IL-6, the mRNA expression of MCP-1 and KC were all detected to a certain extent in all three cell lines in the present study, supporting the reports suggesting that these cytokines are secreted by numerous cell types, including monocytes/macrophages, fibroblasts, and epithelial cells [39, 40]. To our knowledge, our study is the first to show changes in cytokine levels *in vitro* after co-culturing three different cell lines.

Compared to other types of co-culture systems, the multicellular co-culture system has both advantages and limitations. For example, the Transwell chamber culture system or neutralizing cytokine antibodies can be used in the two-cell co-culture system for assessing whether the cell-to-cell interactions are cytokine dependent, and cell behaviors such as migration, proliferation, and phenotype changes can be more easily observed in these systems as the cell types are limited to only two [41, 42]. However, while our multicellular co-culture system is not able to attain these objectives, it more closely resembles the lung microenvironment in terms of the number of different cell types present.

Conclusion

The changes in cytokine levels in our *in vivo* and *in vitro* radiation-induced lung injury models simulating ablative radiotherapy showed unique features, and our findings imply that biological studies related to ADSVI should be investigated using the corresponding experimental models rather than models simulating large-volume CFRT.

Acknowledgments This work was supported by the Nuclear Research and Development Program (NRF-2011-0031695)(JC) and the Radiation Technology R&D program (NRF-2013M2A2A7042978)(JC) through the National Research Foundation of Korea, funded by the Ministry of Science, ICT, and Future Planning; by a faculty research grant from the Yonsei University College of Medicine for 2014 (6-2014-0031)(JC); and by a grant from the Varian Corporation (MDS).

Conflict of interest The authors declare that they have no competing interests.

References

1. Videtic GM, Stephans KL (2010) The role of stereotactic body radiotherapy in the management of non-small cell lung cancer: an emerging standard for the medically inoperable patient? *Curr Oncol Rep* 12(4):235–241

2. Timmerman R, Bastasch M, Saha D, Abdulrahman R, Hittson W, Story M (2007) Optimizing dose and fractionation for stereotactic body radiation therapy. Normal tissue and tumor control effects with large dose per fraction. *Front Radiat Ther Oncol* 40:352–365
3. Timmerman R, McGarry R, Yiannoutsos C, Papiez L, Tudor K, DeLuca J, Ewing M, Abdulrahman R, DesRosiers C, Williams M, Fletcher J (2006) Excessive toxicity when treating central tumors in a phase II study of stereotactic body radiation therapy for medically inoperable early-stage lung cancer. *J Clin Oncol* 24(30):4833–4839
4. Timmerman RD, Story M (2006) Stereotactic body radiation therapy: a treatment in need of basic biological research. *Cancer J* 12(1):19–20
5. Lo SS, Sahgal A, Kunos AC, Teh SB, Yao M, Machtay M, Mayr AN, Huang Z, Chang LE (2012) Reported Toxicities Associated with Stereotactic Body Radiation Therapy. In: Lo SS, Teh BS, Lu JJ, Schefter TE (eds) *Stereotactic Body Radiation Therapy*. Springer, Berlin, pp 373–392
6. Story MD, Nirodi C, Park C (2012) Radiobiology of stereotactic body radiation therapy/stereotactic ablative radiotherapy. In: Lo SS, Teh BS, Lu JJ, Schefter TE (eds) *Stereotactic body radiation therapy*. Springer, Berlin, pp 123–136
7. Hadziahmetovic M, Loo BW, Timmerman RD, Mayr NA, Wang JZ, Huang Z, Grecula JC, Lo SS (2010) Stereotactic body radiation therapy (stereotactic ablative radiotherapy) for stage I non-small cell lung cancer—updates of radiobiology, techniques, and clinical outcomes. *Discov Med* 9(48):411–417
8. Cho J, Kodym R, Selioune S, Richardson JA, Solberg TD, Story MD (2010) High dose-per-fraction irradiation of limited lung volumes using an image-guided, highly focused irradiator: simulating stereotactic body radiotherapy regimens in a small-animal model. *Int J Radiat Oncol Biol Phys* 77(3):895–902
9. Pidikiti R, Stojadinovic S, Speiser M, Song KH, Hager F, Saha D, Solberg TD (2011) Dosimetric characterization of an image-guided stereotactic small animal irradiator. *Phys Med Biol* 56(8):2585–2599
10. Song KH, Pidikiti R, Stojadinovic S, Speiser M, Selioune S, Saha D, Solberg TD (2010) An x-ray image guidance system for small animal stereotactic irradiation. *Phys Med Biol* 55(23):7345–7362
11. Chen Y, Williams J, Ding I, Hernady E, Liu W, Smudzyn T, Finkelstein JN, Rubin P, Okunieff P (2002) Radiation pneumonitis and early circulating cytokine markers. *Semin Radiat Oncol* 12(1 Suppl 1):26–33
12. Mehta V (2005) Radiation pneumonitis and pulmonary fibrosis in non-small-cell lung cancer: pulmonary function, prediction, and prevention. *Int J Radiat Oncol Biol Phys* 63(1):5–24
13. Fleckenstein K, Gauter-Fleckenstein B, Jackson IL, Rabbani Z, Anscher M, Vujaskovic Z (2007) Using biological markers to predict risk of radiation injury. *Semin Radiat Oncol* 17(2):89–98
14. Ao X, Zhao L, Davis MA, Lubman DM, Lawrence TS, Kong FM (2009) Radiation produces differential changes in cytokine profiles in radiation lung fibrosis sensitive and resistant mice. *J Hematol Oncol* 2:6
15. Xie CH, Zhang MS, Zhou YF, Han G, Cao Z, Zhou FX, Zhang G, Luo ZG, Wu JP, Liu H, Chen J, Zhang WJ (2006) Chinese medicine *Angelica sinensis* suppresses radiation-induced expression of TNF-alpha and TGF-beta1 in mice. *Oncol Rep* 15(6):1429–1436
16. Gorshkova I, Zhou T, Mathew B, Jacobson JR, Takekoshi D, Bhattacharya P, Smith B, Aydogan B, Weichselbaum RR, Natarajan V, Garcia JG, Berdyshev EV (2012) Inhibition of serine palmitoyltransferase delays the onset of radiation-induced pulmonary fibrosis through the negative regulation of sphingosine kinase-1 expression. *J Lipid Res* 53(8):1553–1568
17. Rube CE, Wilfert F, Palm J, Konig J, Burdak-Rothkamm S, Liu L, Schuck A, Willich N, Rube C (2004) Irradiation induces a biphasic expression of pro-inflammatory cytokines in the lung. *Strahlenther Onkol* 180(7):442–448
18. Matej R, Housa D, Pouckova P, Zadinova M, Olejar T (2007) Radiation-induced production of PAR-1 and TGF-beta 1 mRNA in lung of C57Bl6 and C3H murine strains and influence of pharmacoprophylaxis by ACE inhibitors. *Pathol Res Pract* 203(2):107–114
19. Rubin P, Johnston CJ, Williams JP, McDonald S, Finkelstein JN (1995) A perpetual cascade of cytokines postirradiation leads to pulmonary fibrosis. *Int J Radiat Oncol Biol Phys* 33(1):99–109
20. Johnston CJ, Hernady E, Reed C, Thurston SW, Finkelstein JN, Williams JP (2010) Early alterations in cytokine expression in adult compared to developing lung in mice after radiation exposure. *Radiat Res* 173(4):522–535
21. Johnston CJ, Manning C, Hernady E, Reed C, Thurston SW, Finkelstein JN, Williams JP (2011) Effect of total body irradiation on late lung effects: hidden dangers. *Int J Radiat Biol* 87(8):902–913
22. Hong ZY, Lee HJ, Choi WH, Lee YJ, Eun SH, Lee JI, Park K, Lee JM, Cho J (2014) A preclinical rodent model of acute radiation-induced lung injury after ablative focal irradiation reflecting clinical stereotactic body radiotherapy. *Radiat Res* 182(1):83–91
23. Hong ZY, Eun SH, Park K, Choi WH, Lee JI, Lee EJ, Lee JM, Story MD, Cho J (2014) Development of a small animal model to simulate clinical stereotactic body radiotherapy-induced central and peripheral lung injuries. *J Radiat Res* 55(4):648–657
24. Anscher MS, Kong FM, Andrews K, Clough R, Marks LB, Bentel G, Jirtle RL (1998) Plasma transforming growth factor beta1 as a predictor of radiation pneumonitis. *Int J Radiat Oncol Biol Phys* 41(5):1029–1035
25. Anscher MS, Peters WP, Reisenbichler H, Petros WP, Jirtle RL (1993) Transforming growth factor beta as a predictor of liver and lung fibrosis after autologous bone marrow transplantation for advanced breast cancer. *N Engl J Med* 328(22):1592–1598
26. Johnston CJ, Piedboeuf B, Baggs R, Rubin P, Finkelstein JN (1995) Differences in correlation of mRNA gene expression in mice sensitive and resistant to radiation-induced pulmonary fibrosis. *Radiat Res* 142(2):197–203
27. Lukacs NW, Hogaboam C, Chensue SW, Blease K, Kunkel SL (2001) Type 1/type 2 cytokine paradigm and the progression of pulmonary fibrosis. *Chest* 120(1 Suppl):5S–8S
28. Shao DD, Suresh R, Vakil V, Gomer RH, Pilling D (2008) Pivotal Advance: Th-1 cytokines inhibit, and Th-2 cytokines promote fibrocyte differentiation. *J Leukoc Biol* 83(6):1323–1333
29. Herzog EL, Bucala R (2010) Fibrocytes in health and disease. *Exp Hematol* 38(7):548–556
30. Sakamoto H, Zhao LH, Jain F, Kradin R (2002) IL-12p40(–/–) mice treated with intratracheal bleomycin exhibit decreased pulmonary inflammation and increased fibrosis. *Exp Mol Pathol* 72(1):1–9
31. Keane MP, Belperio JA, Burdick MD, Strieter RM (2001) IL-12 attenuates bleomycin-induced pulmonary fibrosis. *Am J Physiol Lung Cell Mol Physiol* 281(1):L92–L97
32. Sun L, Louie MC, Vannella KM, Wilke CA, LeVine AM, Moore BB, Shanley TP (2011) New concepts of IL-10-induced lung fibrosis: fibrocyte recruitment and M2 activation in a CCL2/CCR2 axis. *Am J Physiol Lung Cell Mol Physiol* 300(3):L341–L353
33. Westermann W, Schobl R, Rieber EP, Frank KH (1999) Th2 cells as effectors in postirradiation pulmonary damage preceding fibrosis in the rat. *Int J Radiat Biol* 75(5):629–638
34. Gharaee-Kermani M, Nozaki Y, Hatano K, Phan SH (2001) Lung interleukin-4 gene expression in a murine model of bleomycin-induced pulmonary fibrosis. *Cytokine* 15(3):138–147

35. Fajardo LF, Berthrong M (1978) Radiation injury in surgical pathology: part I. *Am J Surg Pathol* 2(2):159–199
36. Moore BB, Kolodsick JE, Thannickal VJ, Cooke K, Moore TA, Hogaboam C, Wilke CA, Toews GB (2005) CCR2-mediated recruitment of fibrocytes to the alveolar space after fibrotic injury. *Am J Pathol* 166(3):675–684
37. Phillips RJ, Burdick MD, Hong K, Lutz MA, Murray LA, Xue YY, Belperio JA, Keane MP, Strieter RM (2004) Circulating fibrocytes traffic to the lungs in response to CXCL12 and mediate fibrosis. *J Clin Invest* 114(3):438–446
38. Brach MA, Gruss HJ, Kaisho T, Asano Y, Hirano T, Herrmann F (1993) Ionizing radiation induces expression of interleukin 6 by human fibroblasts involving activation of nuclear factor-kappa B. *J Biol Chem* 268(12):8466–8472
39. Suga M, Iyonaga K, Ichiyasu H, Saita N, Yamasaki H, Ando M (1999) Clinical significance of MCP-1 levels in BALF and serum in patients with interstitial lung diseases. *Eur Respir J* 14(2):376–382
40. Molls RR, Savransky V, Liu M, Bevans S, Mehta T, Tudor RM, King LS, Rabb H (2006) Keratinocyte-derived chemokine is an early biomarker of ischemic acute kidney injury. *Am J Physiol Renal Physiol* 290(5):1187–1193
41. Li WQ, Li YM, Guo J, Liu YM, Yang XQ, Ge HJ, Xu Y, Liu HM, He J, Yu HY (2010) Hepatocytic precursor (stem-like) WB-F344 cells reduce tumorigenicity of hepatoma CBRH-7919 cells via TGF-beta/Smad pathway. *Oncol Rep* 23(6):1601–1607
42. Milliat F, Francois A, Isoir M, Deutsch E, Tamarat R, Tarlet G, Atfi A, Validire P, Bourhis J, Sabourin JC, Benderitter M (2006) Influence of endothelial cells on vascular smooth muscle cells phenotype after irradiation: implication in radiation-induced vascular damages. *Am J Pathol* 169(4):1484–1495